A&A 418, 305–312 (2004)
DOI: 10.1051/0004-6361:20040035

Astronomy & Astrophysics

On the effect of convection on solar *p* modes

M. Stix and Y. D. Zhugzhda

Kiepenheuer-Institut für Sonnenphysik, Schöneckstr. 6, 79104 Freiburg, Germany

Received 22 April 2003 / Accepted 14 January 2004

Abstract. We investigate the modulation of acoustic wave modes by convection. We consider a cavity that encloses a layer of convection rolls. The stratification due to gravity is taken into account. For the acoustic oscillation we use a harmonic expansion for the horizontal dependence, while a finite-difference scheme is employed in the vertical direction. We calculate the eigenfrequencies of the acoustic modes under adiabatic conditions, as functions of the velocity amplitude of the convection. The results confirm the frequency decreases found in earlier non-stratified models with only a vertical component of the convective velocity.

Key words. convection – Sun: oscillations – methods: analysical

1. Introduction

The frequencies of the solar *p* modes, i.e., the acoustic oscillations that predominantly depend on the restoring force provided by the pressure variation, are almost perfectly reproduced as eigenfrequencies of the standard solar model. Small discrepancies do exist, however, and have been attributed to the imperfect manner of modeling the convection in the layer immediately below the surface. Diverse improvements have been proposed, including modifications of the mean structure of the solar model (Christensen-Dalsgaard & Thompson 1997), and a contribution to the mean pressure caused by the turbulence (Rüdiger et al. 1997; Baturin & Mironova 1998; Rosenthal et al. 1999).

Besides the structural effect, there are direct effects of the fluctuating convective velocity and sound speed on the *p*-mode frequencies (Brown 1984; Zhugzhda & Stix 1994; Stix & Zhugzhda 1998). In this case the frequency change occurs in combination with a modulation of the oscillation amplitude and phase (Stix 2000; Zhugzhda 2002); such effects are visible when the oscillatory velocity field is studied simultaneously with the granular or mesogranular flow (Hoekzema et al. 1998; Hoekzema & Brandt 2000).

An explicit calculation of the convection-oscillation interaction is possible only under simplifying assumptions. The method that we are using was introduced by Kolmogorov who proposed a periodic shear flow as an appropriate "laboratory" to study turbulence (Obuchov 1983). Following this there has been much effort to explore one-dimensional and two-dimensional periodic shear flows (e.g., Takaoka 1989; Frenkel 1991; Thess 1992). But while all these papers were devoted to *incompressible* periodic shear flows, a first step towards *compressible* periodic shear flow is undertaken in the present study. We propose to treat the interplay between acoustic waves and convection by means of a compressible periodic shear flow, in a similar manner as in the earlier incompressible work.

In addition to the variable shear, temperature fluctuations should be included in a model of convection-oscillation interaction. We had already done this in our first one-dimensional periodic model (Zhugzhda & Stix 1994). With that model we were able to demonstrate that the effect of temperature and velocity fluctuations on the phase velocity of acoustic waves has the correct sign to explain the discrepancy between observed and calculated *p*-mode frequencies. The natural next step is to consider a two-dimensional periodic shear flow, which is done in the present paper. Thus we include the horizontal component of the convective flow. Moreover, the present model goes beyond the two earlier models of Zhugzhda & Stix (1994) and Stix & Zhugzhda (1998) in that gravity and the ensuing density and pressure stratification are taken into account.

Of course it would be perfect to consider a shear flow that varies randomly in space and time, accompanied by temperature fluctuations. This was the viewpoint of Brown (1984) when he first concluded that turbulent convection should decrease the solar eigenfrequencies. In the present work we take the opposite view of a regular periodic flow. Probably the solar situation is an intermediate one, between simply periodic and fully stochastic, and it appears that a final quantitative estimate will require three-dimensional numerical simulation; Samadi et al. (2003a,b) and Wedemeyer et al. (2003) have used such simulations to describe the excitation of acoustic oscillations

Send offprint requests to: M. Stix,
e-mail: stix@kis.uni-freiburg.de

by convection. Our present approach is different and simpler: it is an attempt to isolate and better understand a certain physical effect of convection upon the frequencies of oscillation.

In a different view one could consider the coupling of the global oscillations by means of a large-scale time-dependent flow in the convection zone (e.g., Roth & Stix 1999, 2003). However, we shall see that the frequency shift that we investigate in the present model originates near the surface, and a plane-layer model appears to be sufficient.

2. The model and basic equations

Our model consists of a mean stratified atmosphere, into which a sequence of convection rolls is embedded, with period $2d$ and alternating sense of motion, as illustrated in Fig. 1. Such a horizontal sequence of rolls is meant to represent the flow within a certain depth range of the convection zone; the whole convection zone is envisaged as a vertical sequence of layers such as shown in the figure, each with its own characteristic scale, which could be the local pressure scale height. We shall see below that the layer nearest to the surface has the greatest effect on acoustic oscillations.

Cartesian coordinates are used, with x in the horizontal direction, perpendicular to the rolls, and z pointing downwards, parallel to gravity. As the model is two-dimensional, all variables are independent of y, the horizontal direction parallel to the rolls.

Superposed on the convection rolls we shall consider standing acoustic oscillations. Ideally these standing oscillations should be the global p modes of the Sun, and should be determined by the solar structure and the boundary conditions at the center and at the surface. Then, a high radial (spherically symmetric) overtone would have a number of nodal surfaces within our model layer. We suppose that such a situation can be simulated by a mode that is enclosed by the boundaries of the layer, although the nodal surfaces are then at different depths. Therefore, the eigenfrequencies which we calculate below cannot be taken as the solar p-mode frequencies. However, the characteristics of acoustic wave propagation can still be modeled correctly; in particular, the shift that a convective flow produces at a certain given frequency can be estimated.

To derive the equations that describe the convection rolls as well as the equations that govern the acoustic oscillations we start from the general set of hydrodynamic equations, viz.

$$\frac{\partial \rho}{\partial t} + \boldsymbol{V}\cdot\nabla\rho + \rho\,\mathrm{div}\,\boldsymbol{V} = 0, \tag{1}$$

$$\rho\left(\frac{\partial \boldsymbol{V}}{\partial t} + \boldsymbol{V}\cdot\nabla\boldsymbol{V}\right) + \nabla p - \rho\boldsymbol{g} = 0, \tag{2}$$

$$\frac{\partial p}{\partial t} + \boldsymbol{V}\cdot\nabla p + \gamma p\,\mathrm{div}\,\boldsymbol{V} = 0, \tag{3}$$

where $\boldsymbol{V}$, ρ, and p are the dependent variables velocity, density, and pressure; $\boldsymbol{g} = (0, 0, g)$ is the gravitational acceleration (we count z positive *downwards*). Relation (3) expresses the condition of adiabatic changes of state in terms of the Eulerian variables used in this paper; it is equivalent to $\mathrm{d}(p\rho^{\gamma})/\mathrm{d}t = 0$, where $\mathrm{d}/\mathrm{d}t = \partial/\partial t + \boldsymbol{V}\cdot\nabla$.

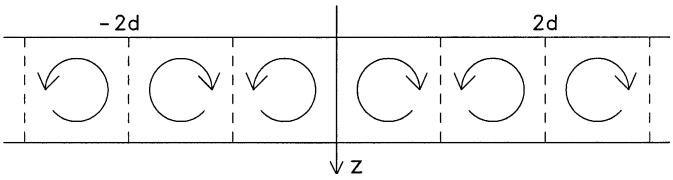

Fig. 1. The model of a layer with convection rolls. The horizontal period is used to define the unit of length, $2d/\pi$.

2.1. Equilibrium state

A subscript 0 will denote the stationary equilibrium state. For this state the equations describing the conservation of momentum, mass, and energy are formally the same as (1)–(3), except that all variables carry a subscript 0, and $\partial/\partial t = 0$. As our model is two-dimensional, the independent space variables are x and z. The continuity equation of the equilibrium state reads $\mathrm{div}\,(\rho_0\boldsymbol{V_0}) = 0$, and in the special case $\rho_0(x, z) = \rho_0(z)$ is reduced to

$$\mathrm{div}\,\boldsymbol{V_0} + \frac{V_{z0}}{H} = 0, \tag{4}$$

where $H(z)$ is the density scale height,

$$H(z) = \left(\frac{1}{\rho_0}\frac{\mathrm{d}\rho_0}{\mathrm{d}z}\right)^{-1}. \tag{5}$$

2.2. Wave equations

Next a small time-dependent perturbation is added to all dependent variables. Since the equilibrium quantities do not depend on time, the time dependence is harmonic, i.e.,

$$\boldsymbol{V}(x, z, t) = \boldsymbol{V_0}(x, z) + \hat{\boldsymbol{v}}(x, z)\,\mathrm{e}^{-\mathrm{i}\omega t}, \tag{6}$$

$$\rho(x, z, t) = \rho_0(x, z) + \hat{\rho}(x, z)\,\mathrm{e}^{-\mathrm{i}\omega t}, \tag{7}$$

$$p(x, z, t) = p_0(x, z) + \hat{p}(x, z)\,\mathrm{e}^{-\mathrm{i}\omega t}. \tag{8}$$

We have decorated the perturbations with a hat in order to distinguish them from the general variables; but we may presently drop the hat without risk of confusion. We substitute these expressions into (1)–(3) and collect the terms that are linear in the perturbations:

$$\rho_0\,(\boldsymbol{V_0}\cdot\nabla\boldsymbol{v} + \boldsymbol{v}\cdot\nabla\boldsymbol{V_0}) + \rho\boldsymbol{V_0}\cdot\nabla\boldsymbol{V_0} + \nabla p - \rho\boldsymbol{g} = \mathrm{i}\omega\rho_0\boldsymbol{v}, \tag{9}$$

$$\boldsymbol{V_0}\cdot\nabla\rho + \rho\,\mathrm{div}\,\boldsymbol{V_0} + \boldsymbol{v}\cdot\nabla\rho_0 + \rho_0\,\mathrm{div}\,\boldsymbol{v} = \mathrm{i}\omega\rho, \tag{10}$$

$$\boldsymbol{V_0}\cdot\nabla p + \gamma p\,\mathrm{div}\,\boldsymbol{V_0} + \boldsymbol{v}\cdot\nabla p_0 + \gamma p_0\,\mathrm{div}\,\boldsymbol{v} = \mathrm{i}\omega p. \tag{11}$$

As an additional simplification of our model we now consider an expansion of all equilibrium quantities in terms of a small parameter that measures the amplitude of the convective velocity. We may choose the Mach number, Ma, for this purpose, and we may define Ma as the ratio of a suitable mean magnitude of the velocity in the convection rolls to a reference value of the sound speed in the layer. If such an expansion is substituted into (1)–(3), and the terms of the diverse orders Ma^n are collected, it becomes clear that the zeroth and first-order contributions to pressure and density do not depend on x, and that, to first order in Ma, the continuity equation has the form (4).

Only in the order Ma^2 the x dependence of ρ_0 and p_0 would enter; here we do not include terms of that order. Thus, the term $\rho \boldsymbol{V_0}\cdot\nabla\boldsymbol{V_0}$ in Eq. (9) will be omitted, and Eqs. (10) and (11) can be simplified by Eq. (4):

$$\boldsymbol{V_0}\cdot\nabla\rho - \rho\,\frac{V_{z0}}{H} + v_z\frac{\rho_0}{H} + \rho_0\,\mathrm{div}\,\boldsymbol{v} = \mathrm{i}\omega\rho, \tag{12}$$

$$\boldsymbol{V_0}\cdot\nabla p - \gamma p\,\frac{V_{z0}}{H} + v_z\frac{dp_0}{dz} + \gamma p_0\,\mathrm{div}\,\boldsymbol{v} = \mathrm{i}\omega p. \tag{13}$$

2.3. Dimensionless variables

In order to introduce dimensionless variables we measure length in terms of $2d/\pi$ and time in terms of $2d/(\pi c_{00})$, where $2d$ is the horizontal period, and c_{00} is the reference value of the sound speed which, in the present model, is the value at the upper boundary of the considered layer. Hence we define

$$\xi = \frac{\pi x}{2d}, \quad \zeta = \frac{\pi z}{2d}, \tag{14}$$

$$C^2(\zeta) = \frac{\gamma p_0}{\rho_0 c_{00}^2}, \quad H(\zeta) = \frac{\pi H(z)}{2d}, \quad \overline{g} = \frac{2dg}{\pi c_{00}^2}, \tag{15}$$

$$V_\xi = \frac{V_{x0}}{c_{00}}, \quad V_\zeta = \frac{V_{z0}}{c_{00}}, \tag{16}$$

$$v_\xi = \frac{v_x}{c_{00}}, \quad v_\zeta = \frac{v_z}{c_{00}}, \tag{17}$$

$$p(\xi,\zeta) = \frac{p(x,z)}{p_0(z)}, \quad \rho(\xi,\zeta) = \frac{\rho(x,z)}{\rho_0(z)}\cdot \tag{18}$$

Here the same symbols denote the dimensional and dimensionless variables H, p, and ρ, but the meaning will always be clear from the context. We introduce

$$\lambda = \frac{2d\,\mathrm{i}\omega}{\pi c_{00}} \tag{19}$$

as a dimensionless frequency. In terms of dimensionless variables the complete set of our wave equations is

$$V_\xi\frac{\partial v_\xi}{\partial\xi} + \frac{\partial V_\xi}{\partial\xi}v_\xi + V_\zeta\frac{\partial v_\xi}{\partial\zeta} + \frac{\partial V_\xi}{\partial\zeta}v_\zeta + \frac{C^2}{\gamma}\frac{\partial p}{\partial\xi} = \lambda\, v_\xi, \tag{20}$$

$$V_\zeta\frac{\partial v_\zeta}{\partial\zeta} + \frac{\partial V_\zeta}{\partial\zeta}v_\zeta + V_\xi\frac{\partial v_\zeta}{\partial\xi} + \frac{\partial V_\zeta}{\partial\xi}v_\xi + \frac{C^2}{\gamma}\frac{\partial p}{\partial\zeta} + \overline{g}(p-\rho) = \lambda\, v_\zeta, \tag{21}$$

$$V_\xi\frac{\partial\rho}{\partial\xi} + V_\zeta\frac{\partial\rho}{\partial\zeta} + \frac{\partial v_\xi}{\partial\xi} + \frac{v_\zeta}{H} + \frac{\partial v_\zeta}{\partial\zeta} = \lambda\,\rho, \tag{22}$$

$$V_\xi\frac{\partial p}{\partial\xi} + V_\zeta\frac{\partial p}{\partial\zeta} + \gamma\, V_\zeta\left(\frac{\overline{g}}{C^2} - \frac{1}{H}\right)p + \frac{\gamma\overline{g}}{C^2}v_\zeta + \gamma\left(\frac{\partial v_\xi}{\partial\xi} + \frac{\partial v_\zeta}{\partial\zeta}\right) = \lambda\, p. \tag{23}$$

For the derivation of these equations we must recall that p and ρ are normalized with the z-dependent equilibrium variables p_0 and ρ_0, cf. Eq. (18).

3. Polytropic atmosphere

Next we specify the equilibrium atmosphere. In the present section we consider a polytropic relation between pressure and density, i.e., $p_0/p_{00} \propto (\rho_0/\rho_{00})^{(N+1)/N}$, where N is the polytropic index, and p_{00} and ρ_{00} refer to the level $z = 0$, the upper boundary of the layer. For a perfect gas in hydrostatic equilibrium the temperature must then be a linear function of depth. For the dimensional variables we obtain the relations

$$T_0 = T_{00} + \beta z, \quad \text{where } \beta = \frac{\mu g}{\mathcal{R}(N+1)}, \tag{24}$$

$$\rho_0 = \rho_{00}(T_0/T_{00})^N, \quad p_0 = p_{00}(T_0/T_{00})^{N+1}, \tag{25}$$

and

$$c_0^2 = c_{00}^2 + \frac{\gamma g z}{N+1}, \quad H = \frac{\mathcal{R}T_0(z)}{\mu g}\left(1 + \frac{1}{N}\right)\cdot \tag{26}$$

The dimensionless coefficients that appear in Eqs. (20)–(23) are determined by

$$C^2(\zeta) = 1 + \frac{\gamma\overline{g}\zeta}{N+1}, \quad H(\zeta) = \frac{1}{\gamma\overline{g}}\left(1 + \frac{1}{N}\right) + \frac{\zeta}{N}\cdot \tag{27}$$

3.1. A special case: Adiabatic stratification

The stratification of the solar convection zone is nearly adiabatic. We now treat this special case, in which the polytropic index is

$$N = \frac{1}{\gamma - 1}\cdot \tag{28}$$

In this case the pressure and density gradients are related by

$$\frac{1}{p_0}\frac{\mathrm{d}p_0}{\mathrm{d}z} = \gamma\frac{1}{\rho_0}\frac{\mathrm{d}\rho_0}{\mathrm{d}z}\cdot \tag{29}$$

The Brunt-Väisälä frequency vanishes; hence internal gravity waves are suppressed. Presently, however, we are interested only in acoustic wave modes. For the dimensionless coefficients of the wave Eqs. (20)–(23) we need the dimensionless sound speed and density scale height,

$$C^2(\zeta) = 1 + (\gamma-1)\overline{g}\zeta\,, \quad H(\zeta) = \frac{1}{\overline{g}} + (\gamma-1)\zeta. \tag{30}$$

Equation (23) can be simplified because now $C^2(\zeta) = \overline{g}H(\zeta)$.

3.2. A system of three equations

In the case of an adiabatic stratification a solution of the wave equations is possible for which

$$p = \gamma\rho, \tag{31}$$

as can be seen from inspection of Eqs. (22) and (23). The meaning of this is that conservation of the specific entropy holds at a *fixed position*, in addition to the specific entropy conservation for a fixed parcel of gas, as expressed by Eq. (3) above. This is an additional constraint to the wave motion, but we expect that the effects that we want to investigate presently, namely those

of the horizontal mean-flow component and of the stratification, are still essentially the same.

Equations (20)–(23) now read

$$V_\xi \frac{\partial v_\xi}{\partial \xi} + \frac{\partial V_\xi}{\partial \xi} v_\xi + V_\zeta \frac{\partial v_\xi}{\partial \zeta} + \frac{\partial V_\xi}{\partial \zeta} v_\zeta + C^2 \frac{\partial \rho}{\partial \xi} = \lambda v_\xi, \tag{32}$$

$$V_\zeta \frac{\partial v_\zeta}{\partial \zeta} + \frac{\partial V_\zeta}{\partial \zeta} v_\zeta + V_\xi \frac{\partial v_\zeta}{\partial \xi} + \frac{\partial V_\zeta}{\partial \xi} v_\xi + C^2 \frac{\partial \rho}{\partial \zeta} + (\gamma - 1)\overline{g}\rho = \lambda v_\zeta, \tag{33}$$

$$V_\xi \frac{\partial \rho}{\partial \xi} + V_\zeta \frac{\partial \rho}{\partial \zeta} + \frac{\partial v_\xi}{\partial \xi} + \frac{1}{H} v_\zeta + \frac{\partial v_\zeta}{\partial \zeta} = \lambda \rho, \tag{34}$$

where C^2 and H, both functions of ζ, have been defined in Eq. (30).

4. The convection rolls. Harmonic expansion

Now the equilibrium velocities are assumed to be

$$V_\xi = U(\zeta) \sin 2\xi, \quad V_\zeta = W(\zeta) \cos 2\xi, \tag{35}$$

where both U and W have amplitudes proportional to the Mach number, Ma. Because of Eq. (4) the two functions are related to each other:

$$U(\zeta) = -\frac{1}{2}\left(\frac{\partial W}{\partial \zeta} + \frac{W}{H(\zeta)}\right). \tag{36}$$

In order to represent convection rolls such as shown in Fig. 1 we specify the dependence on ζ as

$$W(\zeta) = Ma \sin(2\zeta/a), \tag{37}$$

where a is the aspect ratio of the rolls. For $a = 1$ the vertical extent is the same as the horizontal extent, namely $\pi/2$ in the dimensionless and d in the dimensional units; $a < 1$ means rolls with a flat cross-section, $a > 1$ means a vertically elongated cross-section.

4.1. Harmonic expansion

In the following, the dependence of the wave variables on the horizontal coordinate x (or ξ, in the dimensionless form) will be represented in terms of trigonometric functions. Due to the assumed special form Eq. (35) of the convection rolls the dependent variables separate into one set where v_ζ, ρ, and p are symmetric with respect to $\xi = 0$, while v_ξ is antisymmetric, and another set with the opposite symmetry. Without loss of generality we may concentrate on the first set, which we shall call the *symmetric* solution. This solution has the general form

$$v_\xi = \sum_{l=1}^{\infty} u_l(\zeta) \sin 2l\xi, \tag{38}$$

$$v_\zeta = \sum_{l=0}^{\infty} v_l(\zeta) \cos 2l\xi, \tag{39}$$

$$\rho = \sum_{l=0}^{\infty} \rho_l(\zeta) \cos 2l\xi, \tag{40}$$

where the expansion coefficients depend on ζ. After substitution into Eqs. (32)–(34) we obtain an infinite system of coupled ordinary differential equations, in the form of recurrence relations. This is achieved either by means of the addition theorems for the trigonometric functions or, equivalently, by a projection of Eqs. (32)–(34) onto the functions $\cos 2l\xi$ and $\sin 2l\xi$, for all l. These procedures were carried out with the help of the computer algebra package MAPLE. It is necessary to apply care in fixing the initial relations ($l = 0$ and $l = 1$) of the coupled system.

For $l = 2, 3, 4 \ldots$ the following recurrence relations are obtained:

$$l\,U\,(u_{l-1} - u_{l+1}) + \frac{W}{2}\left(\frac{\mathrm{d}u_{l-1}}{\mathrm{d}\zeta} + \frac{\mathrm{d}u_{l+1}}{\mathrm{d}\zeta}\right) + \frac{1}{2}\frac{\mathrm{d}U}{\mathrm{d}\zeta}(v_{l-1} - v_{l+1}) - 2lC^2\rho_l = \lambda u_l, \tag{41}$$

$$W(u_{l-1} - u_{l+1}) + U\Big[(l-2)v_{l-1} - (l+2)v_{l+1}\Big] - \frac{W}{2H}(v_{l-1} + v_{l+1}) + \frac{W}{2}\left(\frac{\mathrm{d}v_{l-1}}{\mathrm{d}\zeta} + \frac{\mathrm{d}v_{l+1}}{\mathrm{d}\zeta}\right) + (\gamma - 1)\overline{g}\rho_l + C^2\frac{\mathrm{d}\rho_l}{\mathrm{d}\zeta} = \lambda v_l, \tag{42}$$

$$U\Big((l-1)\rho_{l-1} - (l+1)\rho_{l+1}\Big) + \frac{W}{2}\left(\frac{\mathrm{d}\rho_{l-1}}{\mathrm{d}\zeta} + \frac{\mathrm{d}\rho_{l+1}}{\mathrm{d}\zeta}\right) + 2\,l\,u_l + \frac{v_l}{H} + \frac{\mathrm{d}v_l}{\mathrm{d}\zeta} = \lambda\rho_l. \tag{43}$$

For the initial equations, $l = 0$ and $l = 1$, we have:

$$-U\,u_2 + \frac{W}{2}\frac{\mathrm{d}u_2}{\mathrm{d}\zeta} + \frac{\mathrm{d}U}{\mathrm{d}\zeta}\left(v_0 - \frac{1}{2}v_2\right) - 2C^2\rho_1 = \lambda u_1, \tag{44}$$

$$-W\,u_1 - \frac{W}{2H}v_1 - 2\,U\,v_1 + \frac{W}{2}\frac{\mathrm{d}v_1}{\mathrm{d}\zeta} + (\gamma - 1)\overline{g}\,\rho_0 + C^2\frac{\mathrm{d}\rho_0}{\mathrm{d}\zeta} = \lambda v_0, \tag{45}$$

$$-W\,u_2 - \frac{W}{H}\left(v_0 + \frac{1}{2}v_2\right) + W\left(\frac{\mathrm{d}v_0}{\mathrm{d}\zeta} + \frac{1}{2}\frac{\mathrm{d}v_2}{\mathrm{d}\zeta}\right) - U(2v_0 + 3v_2) + (\gamma - 1)\overline{g}\,\rho_1 + C^2\frac{\mathrm{d}\rho_1}{\mathrm{d}\zeta} = \lambda v_1, \tag{46}$$

$$-U\,\rho_1 + \frac{W}{2}\frac{\mathrm{d}\rho_1}{\mathrm{d}\zeta} + \frac{v_0}{H} + \frac{\mathrm{d}v_0}{\mathrm{d}\zeta} = \lambda\rho_0, \tag{47}$$

$$-2\,U\rho_2 + W\left(\frac{\mathrm{d}\rho_0}{\mathrm{d}\zeta} + \frac{1}{2}\frac{\mathrm{d}\rho_2}{\mathrm{d}\zeta}\right) + 2\,u_1 + \frac{v_1}{H} + \frac{\mathrm{d}v_1}{\mathrm{d}\zeta} = \lambda\rho_1\,. \tag{48}$$

5. Algebraic eigenvalue problem

The further procedure consists in the introduction of an equidistant grid of ζ values, the formulation of the ζ derivatives in terms of finite differences, and hence in the conversion of the coupled system of differential equations into an algebraic eigenvalue problem. The infinite sums (38)–(40) will be truncated after l_h terms. The matrix whose eigenvalues λ are to be determined has a block structure. The coefficients of variables indexed l in equation l fill the diagonal blocks; the variables indexed $l-1$ and $l+1$ fill the lower and upper sub-diagonal blocks, respectively. The size of the individual blocks is given by the number of grid points in the ζ direction, times the number of equations. Considering that there is no variable u_0 and that for v_l there is one unknown less than for u_l and ρ_l, we see that block number 0 has size $2m_r-1$, while all other blocks have size $3m_r-1$ (cf. Sect. 5.1 below). The truncation index l_h of the harmonic expansion must be chosen such that the eigenvalues (or at least those eigenvalues that are of interest) are nearly independent of that choice. We expect that the necessary l_h will increase with increasing amplitude, Ma, of the convection rolls.

5.1. Boundary conditions and vertical grid

In our model we replace the global acoustic oscillations by standing waves within a layer that is placed at some depth within the convection zone. This renders the model frequencies different from the global p-mode frequencies (a moderate overtone of the layer may represent a high global overtone). Thus, in the present model we apply boundary conditions not for the purpose of calculating eigenfrequencies, but to have definite frequencies available whose shifts by the periodic flow we can then determine.

The simplest boundary condition that fulfills our purpose is to prescribe a node at each of the two surfaces enclosing the layer of convection rolls, $\zeta=0$ and $\zeta=\zeta_1$. Hence we require $v_\zeta=0$ at these two levels, and therefore $v_l(0)=v_l(\zeta_1)=0$ for all l.

The interval $(0,\zeta_1)$ is divided into m_r equal sub-intervals, of length $\Delta\zeta=\zeta_1/m_r$. The unknowns of the problem then consist of the v_l values at the joining points, and of the u_l and ρ_l values at the mid-points of these sub-intervals. Equations (42), (45), and (46) are evaluated at the joining points (except the boundary points $\zeta=0$ and $\zeta=\zeta_1$), the rest of Eqs. (41)–(48) at the interval mid-points. Interpolation between two neighbor points is made when appropriate, and a derivative is represented by a central difference, e.g.,

$$\frac{\mathrm{d}v_l}{\mathrm{d}\zeta}=\frac{v_l(\zeta+\Delta\zeta/2)-v_l(\zeta-\Delta\zeta/2)}{\Delta\zeta}. \tag{49}$$

Near the boundaries, at $\zeta=\Delta\zeta/2$ and $\zeta=\zeta_1-\Delta\zeta/2$, the derivatives of u_l and ρ_l must be represented in one-sided difference form,

$$\frac{\mathrm{d}f}{\mathrm{d}\zeta}=\frac{-3f(\Delta\zeta/2)+4f(3\Delta\zeta/2)-f(5\Delta\zeta/2)}{2\Delta\zeta}$$

for $\zeta=\Delta\zeta/2$, and

$$\frac{\mathrm{d}f}{\mathrm{d}\zeta}=\frac{3f(\zeta_1-\Delta\zeta/2)-4f(\zeta_1-3\Delta\zeta/2)+f(\zeta_1-5\Delta\zeta/2)}{2\Delta\zeta}$$

for $\zeta=\zeta_1-\Delta\zeta/2$; here f stands for u_l or ρ_l.

6. Results

For the numerical determination of the eigenvalues we have used EISPACK routines.

6.1. Analytical test. Coupling of harmonics with $l=1$

We first calculated the eigenfrequencies of a model with $Ma=0$, i.e., in the absence of convection rolls. It is well-known that in this case the solutions can be written in the form of confluent hypergeometric functions. In the special case of plane vertical oscillations these simplify to Bessel functions with fractional index $\gamma/(\gamma-1)$ which, for $\gamma=5/3$, reduces to the even more convenient case of spherical Bessel functions. We have checked our numerical results with this latter case and, for 100 grid points in the interval $(0,\zeta_1)$, found an agreement better that 5×10^{-5} for the lowest eigenvalues, an better than 5×10^{-3} for the higher eigenvalues up to $|\lambda|\approx30$, as considered in the present paper. Of course, still higher eigenvalues are less accurate; and the algebraic formulation of the problem always yields only a finite number of eigenvalues.

Next we allow for coupling of the plane vertical waves, $l=0$, with the first harmonic, $l=1$, i.e., we set $l_\mathrm{h}=1$. This is the minimal non-zero coupling that is possible; it results in two combined modes for each overtone, as shown in Fig. 2. Only near $Ma=0$ these two modes can be identified unambiguously with the original uncoupled modes. As Ma increases the two modes approach each other with *avoided crossings*. Regardless of such avoided crossings, the frequencies show a clear tendency to decrease with increasing amplitude of the convection rolls. Moreover, the higher the frequency, the more pronounced is that decrease. These two findings confirm the results of our earlier models (Zhugzhda & Stix 1994; Stix & Zhugzhda 1998) where only the vertical velocity component was taken into account, and no stratification was considered.

6.2. Harmonics with $l\geq2$

With increasing amplitude of the convection rolls the coupling becomes stronger, and we must see whether the coupling of harmonics with $l\geq2$ affects the results obtained for weak coupling. Figure 3 demonstrates that, as more harmonics are admitted, there are more avoided crossings, and the general appearance of the eigenfrequencies looks confusing at first sight. However, a closer inspection shows that, of each overtone multiplet, the lowest frequency is well represented by harmonics $l\leq1$ up to an amplitude $Ma\approx0.2$, and by harmonics $l\leq2$ up to $Ma\approx0.4$. By and large this agrees with what we had found in the harmonic layer model with only a vertical velocity (Stix & Zhugzhda 1998). As can be seen from the right panel of Fig. 3, there is little interference of the $l=0,1$ pair with the two other modes of the multiplet; only near $Ma=0.5$ such seems to begin, when modes of two neighbored multiplets get almost equal frequencies.

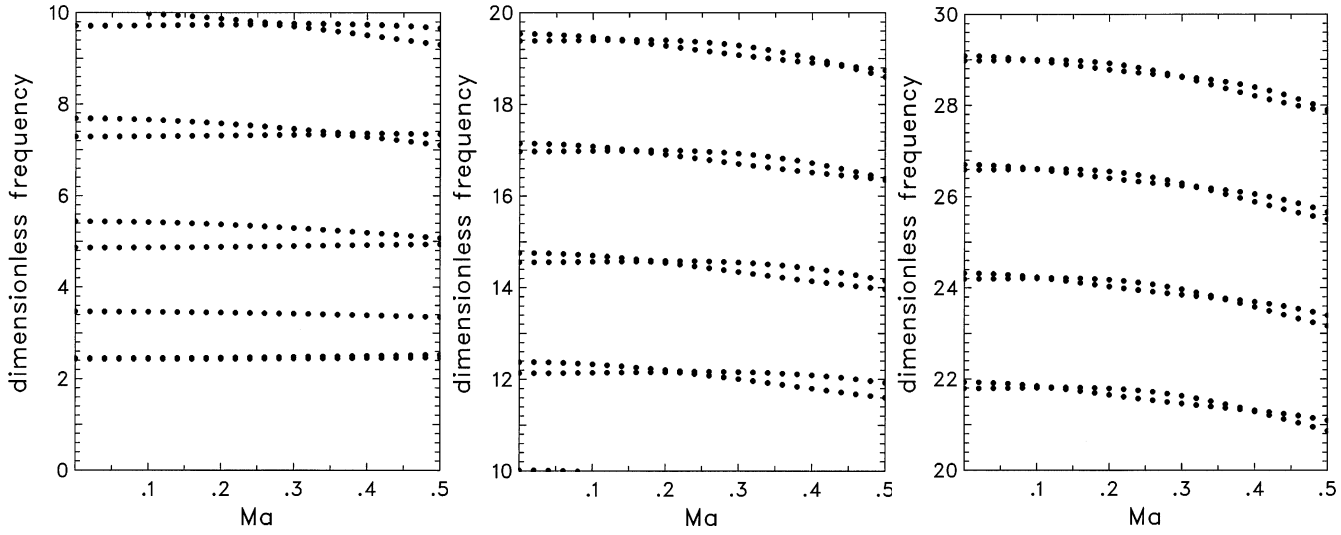

Fig. 2. Dimensionless frequencies, $|\lambda|$, as functions of the amplitude of the convection rolls. The three panels show overtones $n = 0{-}4$ (*left*), $5{-}8$ (*middle*), and $9{-}12$ (*right*); coupling between the harmonics $l = 0$ and $l = 1$ is included. The Mach number Ma is varied in steps of 0.02; continuous curves would avoid crossing each other at a close approach.

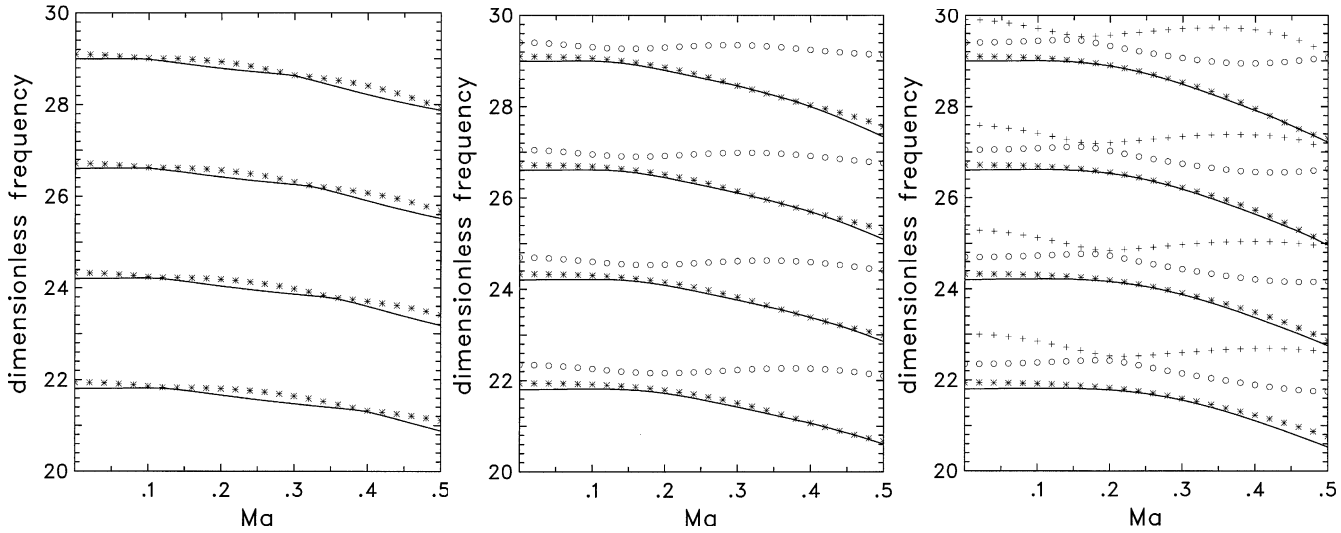

Fig. 3. Coupling of the plane wave ($l = 0$) to horizontal harmonics up to $l = 1$ (*left*), $l = 2$ (*middle*), and $l = 3$ (*right*). The lowest mode of each multiplet is shown as a *dark curve*, the higher modes with *asterisks*, *open circles*, and *crosses*.

Generally our model is restricted to the case of small Mach number Ma. Therefore, the subsequent results have been calculated with a harmonic truncation at $l = 1$. But from Fig. 3 we infer that, qualitatively, the conclusions will be correct even for a somewhat larger roll amplitude.

6.3. The effect of stratification

The stratification of the equilibrium atmosphere is determined by the density scale height (5). At the upper boundary of the layer this scale height is given, in dimensionless units, by Eq. (30):

$$H(0) = 1/\overline{g}. \tag{50}$$

The total variation of the equilibrium density across the layer is derived from Eqs. (24) and (25),

$$\frac{\rho_0(\zeta_1)}{\rho_0(0)} = \left(1 + \frac{\zeta_1}{NH(0)}\right)^N. \tag{51}$$

For $\zeta_1 = \pi/2$ and $N = 1/(\gamma - 1) = 3/2$ this yields a total density variation by factors 1.42 and 5.44 for the choices $H(0) = 4$ and $H(0) = 0.5$, respectively. These are the two cases illustrated in Fig. 4. The results shown in the earlier Figs. 2 and 3 were obtained with $H(0) = 1$, corresponding to a density variation by a factor 2.93.

Figure 4 shows the effect of stratification for the intermediate frequency range, $|\lambda| = 10 \ldots 20$. According to Eq. (27) a stronger stratification (smaller $H(0)$), also implies a larger

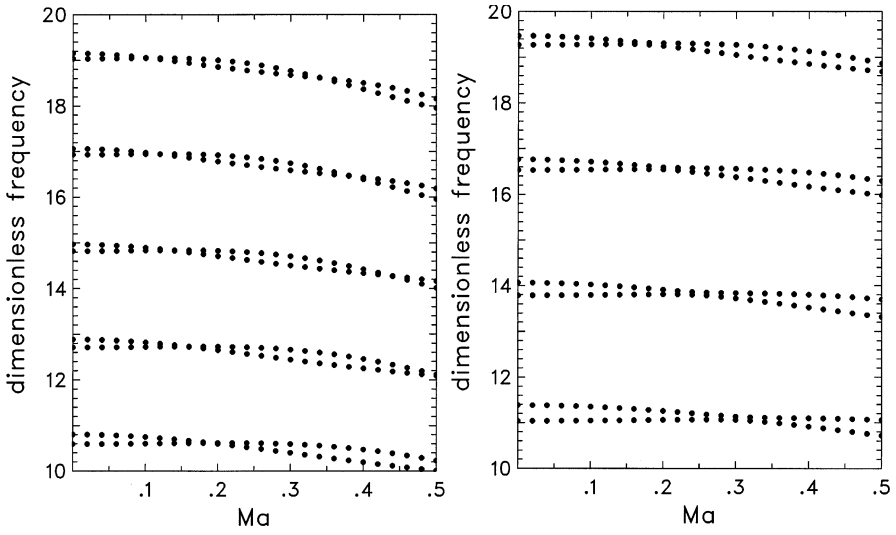

Fig. 4. Eigenfrequencies as in Fig. 1: Weak stratification, with dimensionless density scale height $H(0) = 4.0$ (*left*, overtones $n = 5$–9), and strong stratification, with $H(0) = 0.5$ (*right*, overtones $n = 4$–7).

mean sound speed within the layer and, therefore, correspondingly larger eigenfrequencies. This is the reason for the appearance of different overtone multiplets in the same range of frequencies in two panels of Fig. 4.

As for the effect of convection, it appears that the frequency decrease which is generally observed with increasing convection amplitude becomes weaker when the stratification becomes stronger.

6.4. Flat convection cells

Solar granulation possibly consists of rather *flat* convection cells as, for example, suggested by their horizontal extent, which greatly exceeds typical vertical scales such as the pressure scale height. In order to check whether flat convection cells influence the acoustic oscillation in a different manner than cells with equal vertical and horizontal extent, we have varied the aspect ratio, a, in the definition (37) of $W(\zeta)$. Figure 5 shows the rolls for $a = 0.5$.

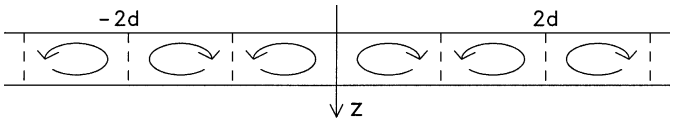

Fig. 5. Layer of flat convection rolls, with aspect ratio $a = 0.5$.

Figure 6 shows the eigenfrequencies as functions of the roll amplitude Ma for the case $a = 0.5$. Because the normalization of length is by means of the horizontal period $2d$ and is unchanged, the vertical extent of the layer is now smaller, and the frequency spacing of the overtone multiplets is larger in proportion to $1/a$. Thus in Fig. 6 we represent the whole range $|\lambda| \leq 30$ in one panel, which contains only overtones up to $n = 6$. This compressed representation at first sight suggests a smaller frequency decrease with increasing Ma than for the rolls of Fig. 1. But a closer look reveals that, at the same frequency, the decrease is in fact larger: at $Ma = 0.5$, it is ≈4.9% for the highest mode shown in Fig. 6, and ≈3.8% for the highest mode of Fig. 2. Again, as with the earlier rolls, the effect increases with increasing frequency, $|\lambda|$.

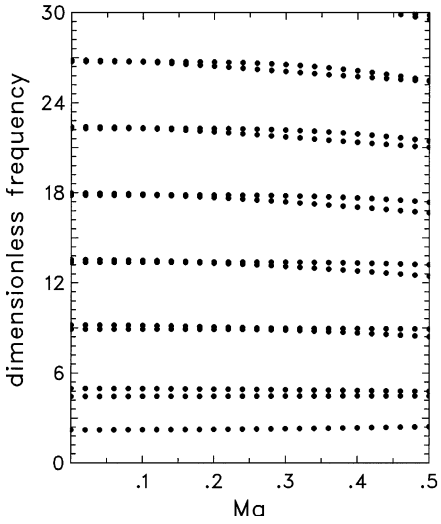

Fig. 6. Dimensionless frequencies as function of the dimensionless amplitude Ma of convection rolls with aspect ratio $a = 0.5$. Note that the frequency drop with increasing Ma is larger than for $a = 1$ (the frequency scale is compressed in comparison to Figs. 2–4).

7. Discussion

We have conceived the present model for the interaction of convection with acoustic oscillations to generalize the results of our earlier, more primitive models. Thus we are able to confirm those earlier results: The convective flow causes a small decrease of the acoustic eigenfrequencies, and this decrease is more pronounced for the higher overtones. Since, in the present model, the horizontal variation of the sound speed has not been taken into account, the frequency decrease is essentially explained by means of the harmonic mean phase velocity for the combined upwards and downwards propagating waves,

$$\bar{v}_{\rm ph} = 2\left(\frac{1}{c_0+V}+\frac{1}{c_0-V}\right)^{-1} \approx c_0\left(1-Ma^2\right) \qquad (52)$$

(Brown 1984; Rosenthal 1997). Indeed, the results shown in the figures above demonstrate the quadratic dependence on Ma. However, as we have pointed out before, the situation is more complicated when c_0 depends on x; in that case the sound-speed and convective-velocity effects reinforce each other for the upwards propagating wave, but oppose each other for the downwards propagating wave.

The influence of the density stratification appears to be small. Strong stratification (small scale height) yields somewhat smaller frequency changes than weak stratification.

A detailed calculation of the frequency correction for p modes of a standard solar model has been made by Zhugzhda & Stix (1994). Their Eq. (61),

$$\frac{\Delta\omega}{\omega} = \frac{\int c_0^{-1}\,\mathrm{d}r}{\int \bar{v}_{\mathrm{ph}}^{-1}\,\mathrm{d}r} - 1, \tag{53}$$

gives the frequency correction in terms of a WKBJ analysis, which yields

$$\frac{\Delta\omega}{\omega} = \frac{\int c_0^{-1}\,\mathrm{d}r}{\int [c_0(1 - Ma(r)^2]^{-1}\,\mathrm{d}r} - 1 \tag{54}$$

if the approximate expression from Eq. (52) is substituted at each radius r.

Equation (54) clearly shows that the frequency correction is negative – a "redshift". It also shows that the largest contribution to the shift comes from the layer nearest to the surface, where Ma reaches its largest value. We expect that, if the convection zone is divided into a stack of layers such as treated in the present paper, and if the effects of all layers on the mean phase velocity are added, the ensuing frequency corrections will be of the right order, as has been estimated by Zhugzhda & Stix (1994) and Stix & Zhugzhda (1998).

For an aspect ratio smaller than 1 we have found larger frequency corrections. This result, too, is consistent with the former models where we had introduced a size factor in order to adapt the layer model to the supposed horizontal size of eddies in the convection zone: A larger size factor meant flat eddies, and resulted in larger frequency corrections.

There are several further steps that should be undertaken following the model of the present paper. The constraint of constant specific entropy (Sect. 3.2) should be relaxed. A variation of c_0 with horizontal coordinate x should be admitted. In addition, it would be worth while to calculate the eigenfunctions (38)–(40), in particular the vertical velocity as a function of x, the horizontal coordinate, and compare it with the Doppler shift of spectral lines originating in the solar atmosphere (Stix 2000; Zhugzhda 2002). In this context a modification of the boundary condition at $z = 0$ appears to be desirable, namely to add an isothermal layer, $z < 0$, to the model, in such a way that the acoustic waves become evanescent in that layer, similar to the solar p modes which are evanescent in the observable layer of the atmosphere.

Finally, a technical remark is appropriate. We have converted the set of linear differential equations into an algebraic eigenvalue problem. Depending on the manner of discretization, spurious eigenvalues may result from such a procedure, at the expense of the highest eigenvalues of the spectrum. We have largely avoided those spurious eigenvalues through the staggered grid described in Sect. 5.1, but for $l_{\mathrm{h}} \geq 2$ some of them still appear. However, due to their dependence on the spacing $\Delta\zeta$, these eigenvalues are easily distinguished and discarded.

Acknowledgements. We are grateful to W. Dobler for a fruitful discussion on the numerical determination of eigenvalues and for reading the manuscript, and to the Deutsche Forschungsgemeinschaft for financial support.

References

Baturin, V. A., & Mironova, I. V. 1998, Structure and Dynamics of the Interior of the Sun and Sun-like Stars, ed. S. Korzennik & A. Wilson, ESA SP-418, Vol. I, 71
Brown, T. M. 1984, Science, 226, 687
Christensen-Dalsgaard, J., & Thompson, M. J. 1997, MNRAS, 284, 527
Frenkel, A. L. 1991, Phys. Fluids A, 3, 1718
Hoekzema, N. M., & Brandt, P. N. 2000, A&A, 353, 389
Hoekzema, N. M., Brandt, P. N., & Rutten, R. J. 1998, A&A, 333, 322
Obuchov, A. M. 1983, Kolmogorov flow and laboratory simulations of it, Russian Math. Survey, 38, 119
Rosenthal, C. S. 1997, Solar convection and oscillations and their relationship, ed. F. P. Pijpers, J. Christensen-Dalsgaard & C. S. Rosenthal (Kluwer), 145
Rosenthal, C. S., Christensen-Dalsgaard, J., Nordlund, Å., Stein, R. F., &Trampedach, R. 1999, A&A, 351, 689
Roth, M., & Stix, M. 1999, A&A, 351, 1133
Roth, M., & Stix, M. 2003, A&A, 405, 779
Rüdiger, G., Hasler, K.-H., & Kitchatinov, L. L. 1997, Astron. Nachr., 318, 173
Samadi, R., Nordlund, Å, Stein, R. F., Goupil, M. J., & Roxburgh, I. 2003a, A&A, 403, 303
Samadi, R., Nordlund, Å, Stein, R. F., Goupil, M. J., & Roxburgh, I. 2003b, A&A, 404, 1129
Stix, M. 2000, Sol. Phys., 196, 19
Stix, M., & Zhugzhda, Y. D. 1998, A&A, 335, 685
Takaoka, M. 1989, J. Phys. Soc. Jpn, 58, 2223
Thess, A. 1992, Phys. Fluids A, 4, 1385
Wedemeyer, S., Freytag, B., Steffen, M., Ludwig, H.-G., & Holweger, H. 2003, A&A, in press
Zhugzhda, Y. D., & Stix, M. 1994, A&A, 291, 310
Zhugzhda, Y. D. 2002, Il Nuovo Cimento C, 25, 623